CHEMISTRY
A EUROPEAN JOURNAL

DOI: 10.1002/chem.200500780

Synthesis of Heterobimetallic Ru–Mn Complexes and the Coupling Reactions of Epoxides with Carbon Dioxide Catalyzed by these Complexes

Man Lok Man,[a] King Chung Lam,[b] Wing Nga Sit,[a] Siu Man Ng,[a] Zhongyuan Zhou,[a] Zhenyang Lin,*[b] and Chak Po Lau*[a]

Abstract: The heterobimetallic complexes $[(\eta^5\text{-}C_5H_5)Ru(CO)(\mu\text{-}dppm)Mn(CO)_4]$ and $[(\eta^5\text{-}C_5Me_5)Ru(\mu\text{-}dppm)(\mu\text{-}CO)_2Mn(CO)_3]$ (dppm = bisdiphenylphosphinomethane) have been prepared by reacting the hydridic complexes $[(\eta^5\text{-}C_5H_5)Ru(dppm)H]$ and $[(\eta^5\text{-}C_5Me_5)Ru(dppm)H]$, respectively, with the protonic $[HMn(CO)_5]$ complex. The bimetallic complexes can also be synthesized through metathetical reactions between $[(\eta^5\text{-}C_5R_5)Ru(dppm)Cl]$ (R = H or Me) and $Li^+[Mn(CO)_5]^-$. Although the complexes fail to catalyze the hydrogenation of CO_2 to formic acid, they catalyze the coupling reactions of epoxides with carbon dioxide to yield cyclic carbonates. Two possible reaction pathways for the coupling reactions have been proposed. Both routes begin with heterolytic cleavage of the Ru–Mn bond and coordination of an epoxide molecule to the Lewis acidic ruthenium center. In Route I, the Lewis basic manganese center activates the CO_2 by forming the metallocarboxylate anion which then ring-opens the epoxide; subsequent ring-closure gives the cyclic carbonate. In Route II, the nucleophilic manganese center ring-opens the ruthenium-attached epoxide to afford an alkoxide intermediate; CO_2 insertion into the Ru–O bond followed by ring-closure yields the product. Density functional calculations at the B3LYP level of theory were carried out to understand the structural and energetic aspects of the two possible reaction pathways. The results of the calculations indicate that Route II is favored over Route I.

Keywords: coupling reactions · cyclic carbonates · density functional calculations · heterobimetallic complexes · reaction mechanisms

Introduction

Bimetallic complexes have attracted much attention because it is believed that with two metal centers in proximity, the reactivity of the individual metal atoms might complement each other and give rise to so-called cooperative reactivity.[1] Moreover, the chemistry of these systems is potentially unique and so they are promising candidates for new chemical and catalytic reactions.[2] Heterobimetallic complexes are of particular interest since it is relatively easy to introduce metal–metal bond polarity into these systems, which can lead to bifunctional activity and direct selectivity in substrate–system interactions. Furthermore, heterolytic cleavage of the polar metal–metal bond in the course of a reaction might generate a metal nucleophile and electrophile pair; the former could act as a Lewis base to activate a substrate and the latter as a Lewis acid to activate a second one. The pair might also activate a polar substrate in a concerted manner.[3]

The utilization of carbon dioxide as a feedstock in the production of chemical products has attracted much attention for economic and environmental reasons.[4] One of the promising methodologies in chemical CO_2 fixation is the coupling of carbon dioxide with epoxides to synthesize cyclic carbonates which are valuable as aprotic polar solvents, fine chemical intermediates, and starting material for the synthesis of polymers and engineering plastics.[5] Various catalysts have been explored for use in such coupling reactions.[6] Some previous reports have suggested that parallel Lewis base activation of CO_2 and Lewis acid activation of

[a] Dr. M. L. Man, W. N. Sit, S. M. Ng, Prof. Z. Zhou, Prof. C. P. Lau
Department of Applied Biology and Chemical Technology
The Hong Kong Polytechnic University
Hung Hom, Kowloon, Hong Kong (China)
Fax: (+852) 2364-9932
E-mail: bccplau@polyu.edu.hk

[b] K. C. Lam, Prof. Z. Lin
Department of Chemistry
The Hong Kong University of Science and Technology
Clear Water Bay, Kowloon, Hong Kong (China)
Fax: (+852) 2358-1594
E-mail: chzlin@ust.hk

Supporting information for this article is available on the WWW under http://www.chemeurj.org/ or from the author. Optimized geometries of all species calculated.

epoxides is important for the success of the reaction.[6a–d] For example, it has been proposed that in the [Cr^{III}salen]/(4-dimethylamino)pyridine (DMAP)-catalyzed CO_2/epoxide coupling reactions, the starting [Cr^{III}salen] complex acts as a Lewis acid to activate the epoxide and the [Cr^{III}salen]·DMAP complex, in which the Cr^{III} center is rendered more electron-rich by the coordination of the DMAP molecule, activates the CO_2 by forming a metallocarboxylate intermediate.[6a] It is also likely that the catalytic activity of Mg–Al mixed oxides in the coupling of carbon dioxide with epoxides originates from the cooperative action of neighboring basic and acidic sites on the surface of the catalyst.[6b] We herein report the synthesis, characterization, and a reactivity study of a pair of Ru–Mn heterobimetallic complexes; the catalysis of the carbon dioxide/epoxide coupling reactions with these complexes has also been investigated.

Results and Discussion

Synthesis and characterization of [(η^5-C_5H_5)Ru(CO)(μ-dppm)Mn(CO)$_4$] (1a) and [(η^5-C_5Me_5)Ru(μ-CO)$_2$(μ-dppm)Mn(CO)$_3$] (1b): We envision that the reaction of the relatively acidic manganese carbonyl hydride [$HMn(CO)_5$] (pK_a (aq scale) = 7.2)[7] with the hydride complex [Cp′Ru(dppm)H] (Cp′ = Cp, Cp*; dppm = bis-diphenylphosphinomethane; the pK_a values (aq scale) of the conjugate acids [CpRu(dppm)(H_2)]$^+$ and [Cp*Ru(dppm)(H_2)]$^+$ are 7.3 and 8.8, respectively)[8] would generate, by elimination of a dihydrogen molecule, the heterobimetallic complex. However, stirring a THF solution of equimolar amounts of [$HMn(CO)_5$] and [Cp′Ru(dppm)H] at room temperature did not seem to lead to the formation of any bimetallic complex. The reaction of the two hydrides in [D_8]THF was therefore monitored by NMR spectroscopy. ^{1}H and ^{31}P{^{1}H} NMR spectroscopy, however, showed that the two hydrides remained unchanged over a period of several hours. The hydride signals of the two hydride complexes remained sharp over a temperature range of 213–293 K, indicative of the absence of stable dihydrogen-bonded bimetallic species Ru–H···H–Mn.[9] The absence of these stable dihydrogen-bonded species in the solution mixture was corroborated by the variable-temperature T_1 relaxation time measurements for the hydride ligand of the ruthenium complex. The T_1(min) values of the hydride ligands of [CpRu(dppm)H] and [Cp*Ru(dppm)H] in [D_5]chlorobenzene were measured to be 1139 ms at 240 K and 924 ms at 244 K, respectively; these values were lowered only slightly to 1099 ms at 247 K and 900 ms at 246 K, respectively, upon addition of one equivalent of [$HMn(CO)_5$] to the solutions.

Despite the seeming absence of stable dihydrogen-bonded species in the solution containing [Cp′Ru(dppm)H] (Cp′ = Cp, Cp*) and [$HMn(CO)_5$], it was, however, learned that H/D exchange occurred upon addition of one equivalent of [$HMn(CO)_5$] to a solution of [Cp′Ru(dppm)D]; an equilibrium in which the deuterium was distributed equally between the two hydride species was established within 30 minutes. With H/D exchange occurring between [Cp′Ru(dppm)D] and [$HMn(CO)_5$], we anticipated that spin-saturation transfer between the two hydride complexes should be observable. It was, however, found that in a solution containing equimolar amounts of [Cp′Ru(dppm)H] and [$HMn(CO)_5$], irradiation of the ruthenium hydride signal did not lead to any enhancement of the hydride signal of the manganese complex. Conversely, the intensity of the ruthenium hydride signal was unaltered when the hydride signal of the manganese complex was irradiated. The hydride exchange between the two complexes is probably much too slow to render the spin-saturation transfer observable.

A mechanism for the H/D exchange between [Cp′Ru(dppm)D] and [$HMn(CO)_5$] is proposed and shown in Scheme 1. The protonic hydrogen of [$HMn(CO)_5$] attacks

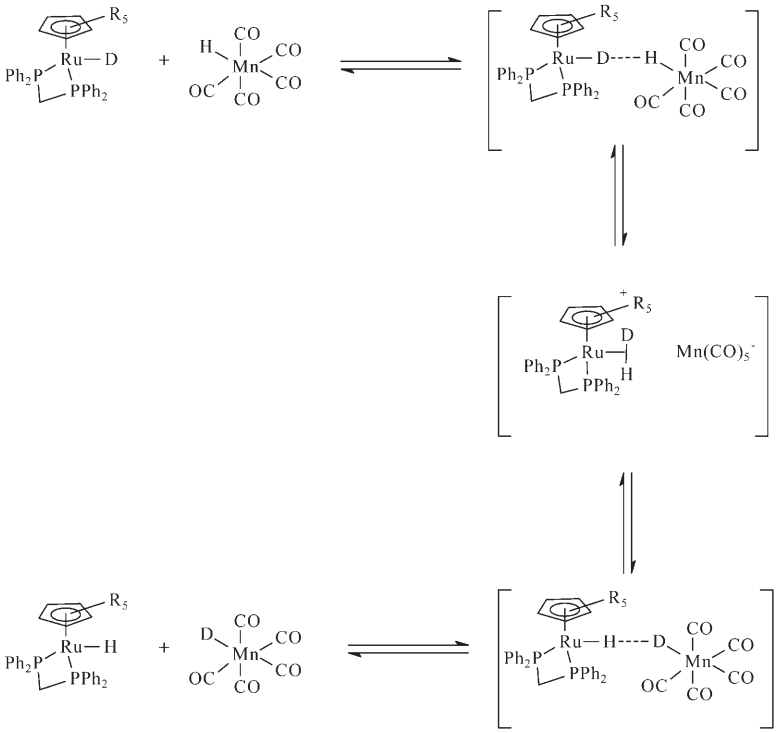

Scheme 1. Proposed mechanism for the H/D exchange between [Cp′Ru(dppm)D] and [$HMn(CO)_5$]. R = H, CH_3.

the deuteride ligand of [Cp′Ru(dppm)D] and H/D exchange proceeds rapidly via the transient intermediates of the Ru–D···H–Mn species and the η^2-HD complex. It has been shown that the kinetic products of the protonation reactions of [Cp′Ru(L_2)H] are the η^2-dihydrogen complexes; depending on the ligands L_2, in some cases, intramolecular tautomerization of the dihydrogen complexes occurs to give the transoid dihydride form or a mixture of dihydrogen and dihydride complexes, while in other cases the η^2-dihydrogen form persists and does not tautomerize to give the dihydride form.[10] Although [Cp′Ru(dppm)H] (Cp′ = Cp or Cp*) and [$HMn(CO)_5$] did not seem to react at room temperature over a period of several hours, it was, however, found that after a [D_8]THF solution of [CpRu(dppm)H]/[$HMn(CO)_5$] (1:1) had been allowed to stand at room temperature in a sealed NMR tube for eight days, the two hydrides had reacted completely to yield the metal–metal-bonded bimetallic complex [CpRu(CO)(μ-dppm)$Mn(CO)_4$] (**1a**) and H_2 [Eq. (1)]. On a preparative scale, **1a** can be prepared by refluxing equimolar amounts of the two hydrides in THF for 15 h. In this reaction the chelating dppm ligand of [CpRu(dppm)H] unwinds upon reaction with [$HMn(CO)_5$] to yield the dppm-bridged complex **1a**.

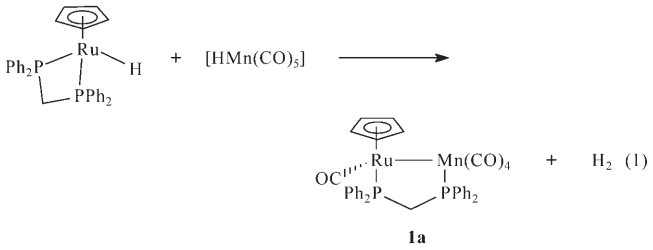

1a

Not unexpectedly, **1a** can also be conveniently prepared by the reaction of the ruthenium chloro complex [CpRu(dppm)Cl] with lithium manganese pentacarbonyls [Eq. (2)]. Similar metathetical reactions have been employed to prepare bimetallic complexes containing metal–metal bonds,[11] including the Ru–Mo and Ru–W bimetallic complexes that we recently reported.[12] It has been suggested that in the heterobimetallic complexes [$RhCo(CO)_3$(μ-dppm)$_2$], [$RhMH(CO)_3$(μ-dppm)$_2$] (M = Fe, Ru, Os), [$RhM(CO)_4$(μ-dppm)$_2$] (M = Mn, Re), and [$RhMH(CO)_4$(μ-dppm)$_2$] (M = Cr, W), the metal–metal bonds are M→Rh^I dative bonds.[13] It has also been reported that the heterobimetallic complex formed by the metathetical reaction of Li^+[η^5-$C_5H_4P(C_6H_4$-*p*-$CH_3)_2Mo(CO)_4]^-$ with [{(C_6H_4-*p*-CH_3)PCH_2}RhCl]$_2$ contains a highly polarized $Rh^{\delta+}$–$Mo^{\delta-}$ bond; changing the donating phosphine ligands on rhodium to carbonyls led to a reduction of the metal–metal-bond polarity.[14] The bimetallic complex [(PEt_3)$_2$(CO)Rh–$Co(CO)_4$] has been shown to possess a polar metal–metal bond which structurally and chemically is best described as a Rh^I–Co^{-I} complex in which the $[Co(CO)_4]^-$ group behaves as a pseudo-halide.[3f] It seems reasonable to regard the manganese moiety in **1a** as a pseudo-halide that forms a dative Mn→Ru bond with a formulation of Ru^{II}/Mn^{-I}.

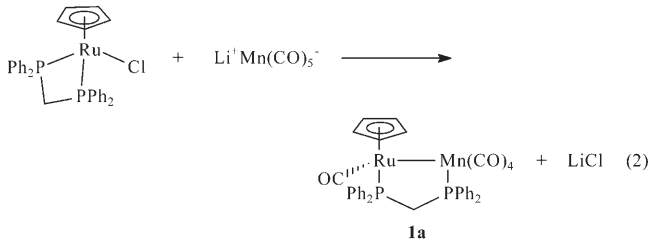

1a

The $^{31}P\{^1H\}$ NMR spectrum of **1a** exhibits a pair of doublets at $\delta = 54.9$ and 56.6 ppm [$^2J(P,P) = 91.2$ Hz]. The methylene hydrogen atoms of the dppm ligand appear as a triplet at $\delta = 2.90$ ppm [$J(H,P) = 9.91$ Hz] in the ^1H NMR spectrum. These hydrogen atoms should, in principle, be diastereotopic, they are magnetically equivalent and have basically identical coupling constants to the two phosphorus atoms, probably by coincidence. Complex **1a** exhibits three carbonyl peaks at 247.0, 225.6, and 222.5 ppm (relative intensities, 2:2:1) in the ^{13}C NMR spectrum. The IR spectrum (KBr) of the complex shows, in addition to the bands at 1896, 1938, and 2000 cm^{-1} due to terminal carbonyl groups, a relatively low-energy CO stretching frequency at 1710 cm^{-1}. The presence of this low CO stretching frequency indicates that a bridging or semibridging carbonyl group is present in the bimetallic complex. Our recently reported Ru–Mo and Ru–W heterobimetallic complexes, which contain semibridging carbonyl ligands, exhibit low-energy CO stretching frequencies at 1777–1792 cm^{-1}.[12]

Similar to **1a**, the pentamethylcyclopentadienyl analog, [{η^5-$C_5(CH_3)_5$}Ru(μ-CO)$_2$(μ-dppm)$Mn(CO)_3$] (**1b**) (vide infra) was prepared by the reaction of the two hydride precursors or by the metathetical reaction. The $^{31}P\{^1H\}$ NMR spectrum of **1b** shows two doublets at $\delta = 48.1$ [$^2J(P,P) = 105.0$ Hz] and 51.2 ppm [$^2J(P,P) = 105.0$ Hz]. Similar to those of **1a**, the methylene hydrogen atoms of the bridging dppm ligand of **1b** also appear as a triplet [$\delta = 2.35$ ppm; $J(H,P) = 9.1$ Hz] in the ^1H NMR spectrum. The complex shows only two carbonyl peaks at $\delta = 269.8$ and 225.6 ppm (relative intensities, 3:2) in the ^{13}C NMR spectrum. The IR spectrum (KBr) of **1b**, in addition to the bands due to terminal carbonyl groups, exhibits a low-energy CO stretch at 1710 cm^{-1}, which might be due to semibridging or bridging carbonyl groups.

Molecular structures of 1a and 1b: The metal–metal-bonded bimetallic structure of **1a** was confirmed by X-ray crystallography. The molecular structure of **1a** is shown in Figure 1 (the solvent molecule CH_2Cl_2, which is disordered, is not shown). The crystal data and refinement details are given in Table 1. Selected bond distances and angles are given in Table 2. The Ru–Mn bond distance of 2.8524(7) Å in **1a** is comparable to the metal–metal bond lengths measured in other Ru–Mn bimetallic complexes that contain bridging ligands, for example, [RuMn(μ-H)(μ-PPh_2)(η^5-

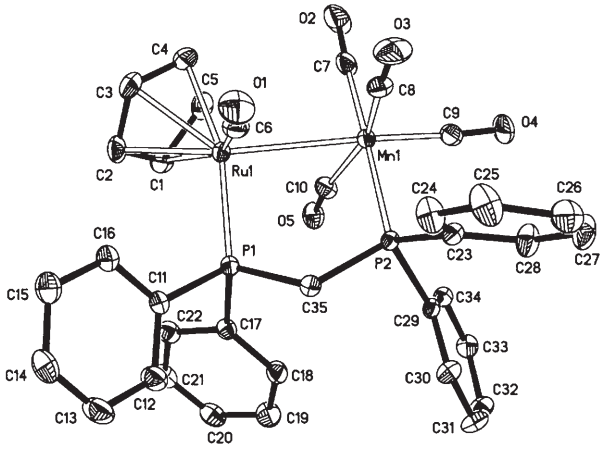

Figure 1. X-ray structure of $[(C_5H_5)Ru(CO)(\mu\text{-dppm})Mn(CO)_4]$ (**1a**).

Table 1. Crystal data and structure refinement for complexes **1a·0.5 CH_2Cl_2** and **1b**.

	1a·0.5 CH_2Cl_2	**1b**
empirical formula	$C_{35.5}H_{28}ClMnO_5P_2Ru$	$C_{40}H_{37}MnO_5P_2Ru$
formula weight	787.98	815.65
temperature [K]	294(2)	294(2)
wavelength [Å]	0.71073	0.71073
crystal system	monoclinic	orthorhombic
space group	$P2_1/c$	$P2_12_12_1$
unit cell dimensions		
a [Å]	18.813(3)	11.7144(15)
b [Å]	10.5259(14)	13.1309(18)
c [Å]	19.633(3)	24.014(3)
α [°]	90	90
β [°]	90	90
γ [°]	90	90
volume [Å^3]	3617.5(11)	3693.8(8)
Z	4	4
ρ_{calcd} [Mg m^{-3}]	1.429	1.467
μ [mm^{-1}]	0.955	0.880
F(000)	1588	1664
crystal size [mm^3]	0.22×0.20×0.14	0.30×0.16×0.14
θ range [°] for data collection	2.11–27.54	2.48–27.52
index ranges		
	$-23 \leqq h \leqq 24$	$-12 \leqq h \leqq 15$
	$-13 \leqq k \leqq 13$	$-17 \leqq k \leqq 13$
	$-25 \leqq l \leqq 10$	$-31 \leqq l \leqq 30$
reflections collected	24254	25195
independent reflections	8410 [R(int) = 0.0363]	8468 [R(int) = 0.0365]
completeness to θ = 27.64° [%]	99.6	99.7
absorption correction	empirical	empirical
max. and min. transmission	0.8779 and 0.8174	0.8867 and 0.7782
refinement method	full-matrix least-squares on F^2	full-matrix least-squares on F^2
data/restraints/parameters	8410/6/417	8468/0/447
goodness-of-fit on F^2	1.032	1.019
final R indices [$I > 2\sigma(I)$]	R_1 = 0.0468, wR_2 = 0.129	R_1 = 0.0320, wR_2 = 0.0548
R indices (all data)	R_1 = 0.0742, wR_2 = 0.1439	R_1 = 0.0434, wR_2 = 0.0575
largest diff. peak and hole [e Å^{-3}]	0.858 and −0.436	0.596 and −0.416

Table 2. Selected bond lengths and angles for $[(C_5H_5)Ru(CO)(dppm)Mn(CO)_4]$ (**1a**).

interatomic distances [Å]			
Ru1–Mn1	2.8524(7)	Ru1–P1	2.2842(10)
Mn1–P2	2.2894(11)	Ru1–C6	1.832(5)
Mn1–C7	1.801(5)	Mn1–C8	1.839(5)
Mn1–C9	1.793(5)	Mn1–C10	1.832(4)
O1–C6	1.158(6)	O2–C7	1.145(5)
O3–C8	1.130(5)	O4–C9	1.152(5)
O5–C10	1.157(5)		
intramolecular angles [°]			
C35-P1-Ru1	112.32(12)	C35-P2-Mn1	113.75(12)
O1-C6-Ru1	171.7(4)	O2-C7-Mn1	176.0(6)
O3-C8-Mn1	176.3(5)	O4-C9-Mn1	176.1(4)
O5-C10-Mn1	167.3(4)		

$C_5H_5)(CO)_5]$, in which the Ru–Mn bond length is 2.894(1) Å;[15] it is, however, shorter than those of the Ru–Mn bimetallic complexes that have no bridging ligands, such as the α-diimine Ru–Mn bimetallic complex $[(CO)_5Mn–Ru(Me)(CO)_2(\alpha\text{-diimine})]$ [α-diimine = pyridine-2-carbaldehyde-*N*-isopropylimine (*i*Pr-PyCa)], in which the Ru–Mn bond distance was found to be 2.9875(8) Å.[16] Note that for one of the carbonyl ligands attached to the manganese center, the Mn-C-O angle [Mn1-C10-O5, 167.3(4)°] deviates more from linearity than those of the other CO ligands on the manganese atom. Moreover, the distance of the carbon atom of this less linear carbonyl ligand on manganese from the ruthenium center measures 2.656(4) Å; this relatively short distance is indicative of the presence of a weak interaction between this CO group and the ruthenium center. In a Zr–Ru bimetallic complex, the zirconium-bound CO, which is slightly bent (Zr-C-O, 167°), semibridges the ruthenium center and the carbon atom of the bent CO is 2.70 Å from the ruthenium center.[17] Moreover, in each of the Ru–M (M = Mo, W) bimetallic complexes, one of the metal-bound CO ligands is a semibridging carbonyl, the M-C-O angle deviates significantly from linearity, and the distance of the carbon atom of this carbonyl ligand from the ruthenium center falls in the range of 2.744–2.906 Å.[12]

Figure 2 shows the X-ray structure of **1b**. The crystal data and refinement details are included in Table 1. Selected bond lengths and angles are given in Table 3. An obvious difference between the structure of **1b** and that of **1a** is that the former contains two bridging carbonyl groups, whilst the latter contains only one semibridging CO. Both bridging carbonyl ligands in **1b** lean slightly towards the ruthenium center. The Ru–Mn bond length in **1b** is, as expected, shorter than that of **1a** (2.7777(5) Å versus 2.8524(7) Å) as a result of the presence of two bridging carbonyl groups. The C–O bond lengths of the bridging carbonyls are significantly longer than those of the terminal CO ligands in the complex.

Reactions of 1a and 1b with H_2/CO_2: We have studied dihydrogen-bonding interactions in aminocyclopentadienylruthenium complexes and have learned that complexes containing intramolecular Ru–H···H–N dihydrogen bonds catalyze CO_2

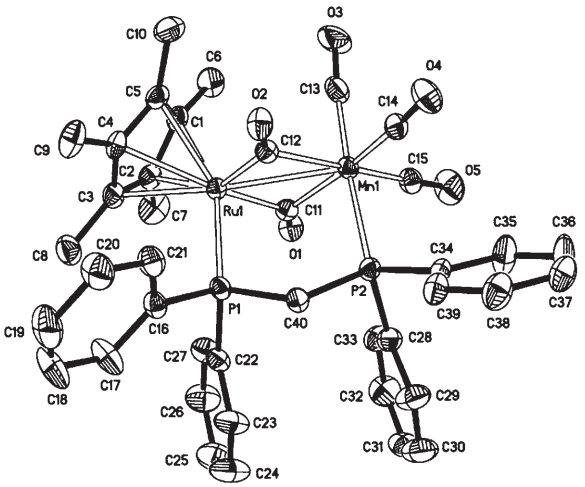

Figure 2. X-ray structure of $[\{C_5(CH_3)_5\}Ru(\mu\text{-}CO)_2(\mu\text{-}dppm)Mn(CO)_3]$ (**1b**).

Table 3. Selected bond lengths and angles for $[\{C_5(CH_3)_5\}Ru(\mu\text{-}CO)_2(\mu\text{-}dppm)Mn(CO)_3]$ (**1b**).

interatomic distances [Å]			
Ru1-Mn1	2.7777(5)	Ru1-P1	2.2969(8)
Mn1-P2	2.3296(9)	Ru1-C11	1.994(3)
Ru1-C12	1.950(3)	Mn1-C11	2.096(3)
Mn1-C12	2.151(3)	Mn1-C13	1.804(4)
Mn1-C14	1.820(3)	Mn1-C15	1.792(3)
O1-C11	1.178(3)	O2-C12	1.190(3)
O3-C13	1.153(4)	O4-C14	1.136(3)
O5-C15	1.153(3)		
intramolecular angles [°]			
P1-Ru1-Mn1	93.55(2)	P2-Mn1-Ru1	93.09(2)
Ru1-C12-Mn1	85.13(11)	P2-C40-P1	112.78(15)
O1-C11-Ru1	137.0(2)	O1-C11-Mn1	136.7(2)
O2-C12-Ru1	141.1(2)	O2-C12-Mn1	133.6(2)

hydrogenation to yield formic acid, albeit in low yields. During the catalytic reaction, the dihydrogen-bonded moiety plays an important role in transferring the hydrogen atoms of H_2 to the CO_2 molecule.[18] More recently we studied the promoting effects of water and alcohols on CO_2 hydrogenation reactions catalyzed by the hydrotris(pyrazolyl)-borato (Tp) ruthenium hydride complex $[TpRu(PPh_3)(CH_3CN)H]$; supported by theoretical calculations, we proposed that the active species is the aquo or alcohol hydride complex $[TpRu(PPh_3)(ROH)H]$ (R = H or alkyl), which is a bifunctional catalyst that transfers the metal hydride and the proton of the coordinated ROH molecule to the carbon and oxygen atoms of the CO_2 molecule, respectively, in a concerted manner; that is, the CO_2 molecule does not have to coordinate to the metal center.[19] One of our interests in this work was to study the reactivity of the bimetallic complexes towards H_2 in the hope of generating dihydrogen-bonded bimetallic species that might act as bifunctional catalysts capable of delivering a H^+ and a H^- in a concerted process (Scheme 2). The bimetallic species are reminiscent of metal–ligand bifunctional catalysts such as the Shvo catalyst[20] and the chiral "metal/NH" catalysts reported by Noyori[21] and Morris[22] and their co-workers. We therefore monitored the reactions of **1a** and **1b** with H_2 by $^{31}P\{^1H\}$ NMR spectroscopy. It was, however, found that after heating a C_6D_6 solution of **1a** or **1b** at 100 °C in a high-pressure NMR tube under about 35 atm of H_2 for 45 h, the complex remained unchanged. Attempted CO_2 hydrogenation (CO_2/H_2 = 35 atm/35 atm; 100 °C for 45 h) with **1a** or **1b** in the presence of Et_3N in an autoclave was also unsuccessful, that is, no $HCOOH{\cdot}Et_3N$ adduct was detected.

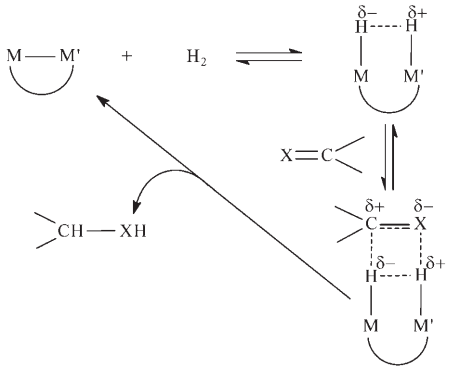

Scheme 2.

Carbon dioxide/epoxide coupling reactions with 1a and 1b: Although **1a** and **1b** are not catalytically active in the hydrogenation of carbon dioxide, it was, however, found that they are active in catalyzing the coupling reactions of carbon dioxide with epoxides to give cyclic carbonates. The results of these reactions are shown in Table 4. The catalytic reactions were carried out in neat epoxides and no CO_2/epoxide copolymer was formed in any of the reactions. After the removal of the product and the unreacted substrate from the catalytic reaction mixture, ^1H and $^{31}P\{^1H\}$ NMR spectroscopy showed that the bimetallic complex was recovered unchanged.

Note that the presence of electron-withdrawing groups on the epoxides leads to higher conversions (Table 4, entries 1–4). The failure of styrene oxide and cyclohexene oxide to couple with CO_2 is probably due to steric congestion. In general, complex **1b** has a lower catalytic activity than **1a**; the lower activity of **1b** might be attributable to greater steric hindrance and the presence of two bridging carbonyl groups which render the cleavage of the metal–metal bond a more demanding step (vide infra).

We have also studied the catalytic activity of the individual metallic moieties of the complexes in CO_2/epoxide coupling reactions. It was found that the ruthenium complexes $[(\eta^5\text{-}C_5H_5)Ru(CO)(PPh_3)(CH_3CN)]OTf$ and $[(\eta^5\text{-}C_5H_5)Ru(CO)(PPh_3)(Cl)]/Ag^+OTf^-$ were inactive in the reaction, however, the manganese complex $Li[Mn(CO)_4(PPh_3)]$ (**1c**) was found to be active, its activity in general being lower than that of **1a** but comparable to that of **1b**. The results of the **1c**-catalyzed CO_2/epoxide coupling reactions are also included in Table 4. In general, the activities

Table 4. Catalytic coupling reactions of CO_2 and epoxides.[a]

Entry	Substrate	Catalyst	TON[b]	TOF[c]	Entry	Substrate	Catalyst	TON[b]	TOF[c]
1	epifluorohydrin	**1a**	8640	216	14	butadiene monoxide	**1b**	1940	48
2	epichlorohydrin	**1a**	8000	200	15	1,2-epoxyhexane	**1b**	120	3
3	epibromohydrin	**1a**	6450	161	16	cyclohexene oxide	**1b**	trace	trace
4	propylene oxide	**1a**	1490	37	17	epifluorohydrin	**1c**	7020	176
5[d]	propylene oxide	**1a**	trace	trace	18	epichlorohydrin	**1c**	5400	135
6	butadiene monoxide	**1a**	2800	70	19	epibromohydrin	**1c**	4100	103
7	1,2-epoxyhexane	**1a**	480	12	20	propylene oxide	**1c**	440	11
8	cyclohexene oxide	**1a**	trace	trace	21[d]	propylene oxide	**1c**	trace	trace
9	epifluorohydrin	**1b**	7050	176	22[e]	propylene oxide	**1c**	trace	trace
10	epichlorohydrin	**1b**	5300	132	23	butadiene monoxide	**1c**	1795	45
11	epibromohydrin	**1b**	4200	105	24	1,2-epoxyhexane	**1c**	110	3
12	propylene oxide	**1b**	450	11	25	cyclohexene oxide	**1c**	trace	trace
13[d]	propylene oxide	**1b**	trace	trace					

[a] Typical reaction conditions: 3.5 μmol catalyst, 31.5 mmol substrate (S/C = 9000), 40 bar CO_2 pressure, 100 °C, 40 h. [b] Turnover number (TON) = no. of moles of product/no. of moles of catalyst. [c] Turnover number frequency (TOF) = TON/time(h). [d] 7.0 μmol of CH_3CN added. [e] 7.0 μmol of [12]crown-4 added.

of **1a** and **1b** are similar to those of Cr^{III},[6a] Zn^{II},[6m] Cu^{II},[6m] and Co^{II}[6m] salen-type complexes and $[Re(CO)_5Br]$.[6o] Complexes **1a** and **1b**, however, exhibit much higher catalytic activities in the coupling reactions of epihalohydrins with CO_2. Note that in general the catalytic activity of the less well-defined $[Ni(PPh_3)_2Cl_2]/PPh_3/Zn/n\text{-}Bu_4NBr$ system[6k] is more than an order of magnitude higher than those of **1a** and **1b**.

Proposed mechanism for the catalytic CO_2/expoxide coupling reaction: It has been proposed that the coupling of epoxides with carbon dioxide to yield cyclic carbonates probably requires the activation of both substrates; the former by a Lewis acid and the latter by a Lewis base.[6a–d] Route I of Scheme 3 shows a possible mechanism for the **1a**-catalyzed CO_2/epoxide coupling reactions. Heterolytic cleavage of the metal–metal bond generates an electrophilic ruthenium fragment and a nucleophilic manganese moiety. An epoxide molecule then coordinates to the Lewis acidic ruthenium center, whilst the Lewis basic manganese center activates the carbon dioxide by forming a metallocarboxylate anion. Although not isolated, the manganese carboxylate $[Mn(CO)_4(PPh_3)(CO_2)]^-$ was believed to be the intermediate in the reaction of $K[CpFe(CO)(PPh_3)(CO_2)]$ with $[Mn(CO)_5(PPh_3)]BF_4$ followed by the addition of CH_3I to afford $[CpFe(CO)_2(PPh_3)]BF_4$ and $[Mn(CO)_4(PPh_3)(CH_3)]$.[23] Nucleophilic ring-opening of the ruthenium-attached epoxide by the manganese carboxylate in Scheme 3 generates **A** which then extrudes the cyclic carbonate by ring-closure. It is widely accepted that coordination of an epoxide molecule to a Lewis acid facilitates nucleophilic ring-opening of the former.[24] The proposed epoxide complex and the ring-opened species in Route I of Scheme 3 are probably transient intermediates because we have not been able to detect either of these species in NMR-monitored catalytic CO_2/propylene oxide coupling reactions carried out in 10 mm sapphire high-pressure NMR tubes. We have also failed to isolate or detect any epoxide complex in independent studies involving the reactions of $[(\eta^5\text{-}C_5H_5)Ru(PPh_3)(CO)(CH_3CN)]^+$ and $[(\eta^5\text{-}C_5H_5)Ru(PPh_3)(CO)(Cl)]/Ag^+OTf^-$ with propylene oxide. The fact that the addition of a small amount of CH_3CN, which is a much better coordinating ligand to ruthenium than propylene oxide, completely quenches the catalytic reaction (Table 4, entry 5) lends support to the notion that activation of the epoxide by the electrophilic ruthenium center is crucial to the success of the coupling reaction. The **1b**-catalyzed coupling reaction could probably proceed by the same mechanism, although the cleavage of the Ru–Mn metal–metal bond, which is flanked by two bridging carbonyl groups, might be a more demanding step. Moreover, **1b** is more hindered than **1a**.

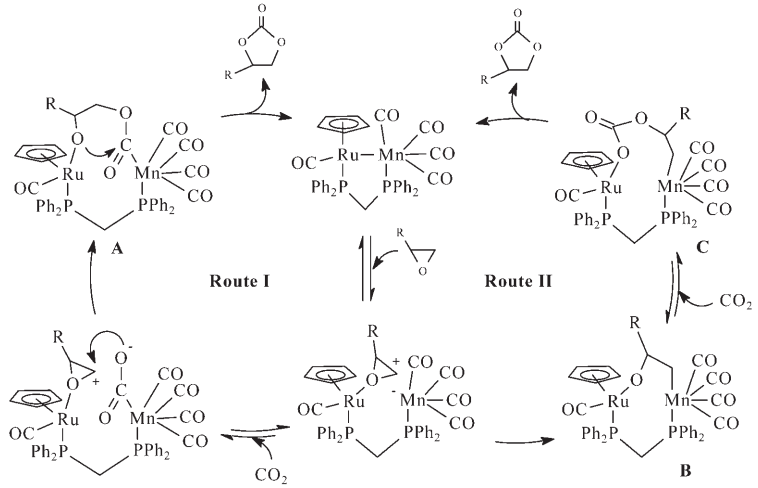

Scheme 3.

An alternative mechanism for the CO_2/epoxide coupling reaction is also proposed (Scheme 3, Route II). In this proposed mechanism, the manganese fragment, instead of forming a metallocarboxylate with CO_2, ring-opens the epoxide, which is activated by O-coordination to the ruthenium fragment, to form the cyclic alkoxide **B**. CO_2 then inserts into the Ru–O bond to form the cyclic metal carbonate **C**, which then extrudes the cyclic carbonate. The insertion of CO_2 into a metal–alkoxide bond to form a metal carbonate species is well-documented.[25]

The lithium salt of the manganese tetracarbonylate anion $Li[Mn(CO)_4(PPh_3)]$ (**1c**) was shown to be an active catalyst in the coupling reactions, although, in general, its activity is lower than that of **1a** (Table 4). The lithium cation of **1c** is probably capable of activating the epoxide by attaching to the oxygen atom of the latter. The fact that the addition of acetonitrile (Table 4, entry 21) or 12-crown-4 (Table 4, entry 22), which is able to solvate or encapsulate Li^+, respectively, practically quenches the activity of **1c** gives credence to this premise. It has been reported that benzo[15]-crown-5 acts as a deactivator in sodium halide catalyzed CO_2/epoxide coupling reactions; the crown ether is a good host for the sodium cation.[6j] The proximity of the metal centers in **1a** is an advantage over **1c**.

Computational study: To understand the structural and energetic aspects of the possible reaction pathways proposed above for the carbon dioxide/epoxide coupling reactions catalyzed by Ru–Mn heterobimetallic complexes, theoretical calculations at the B3LYP level of density functional theory were carried out. In our calculations, the model catalyst $[(\eta^5\text{-}C_5H_5)Ru(CO)(\mu\text{-dppm})Mn(CO)_4]$ was used in which the phenyl groups in the dppm ligand were replaced by hydrogen atoms. The two proposed reaction pathways (Routes I and II in Scheme 3) were studied. For the convenience of our discussion, all the calculated structures of the intermediates, reactants, and transition states are numbered and the transition states are labelled with **TS**.

Coupling reaction of carbon dioxide and ethylene oxide: Figure 3 shows the two possible reaction pathways (Routes I and II) for the carbon dioxide/epoxide coupling reaction; the relative free energies and electronic energies (in parentheses) are also shown. To take into account the effect of entropy, we use the free energies rather than the electronic energies in our discussion because two or more molecules are involved in the reactions studied herein. For the reader's information, the relative electronic energies are also shown in parentheses in Figure 3.

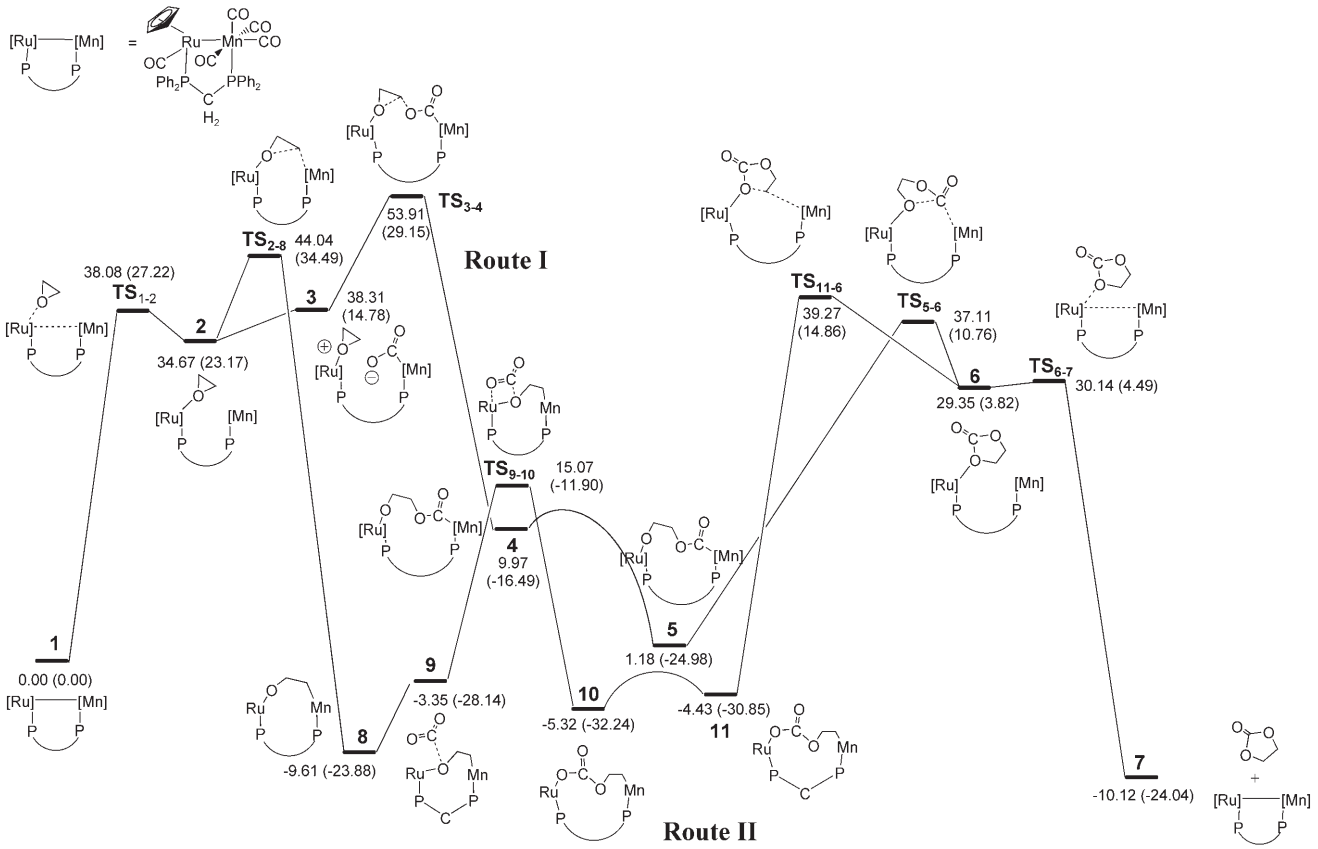

Figure 3. Schematic illustration of the two reaction pathways studied in the coupling reaction of carbon dioxide with ethylene oxide. The calculated relative free energies (kcal mol^{-1}) and the relative electronic energies (in parentheses) of the species involved in the reaction are given. The relative energies of all species are given relative to $[(\eta^5\text{-}C_5H_5)Ru(CO)(\mu\text{-dppm})Mn(CO)_4]$, CO_2, and C_2H_4O.

Both Routes I and II begin with a bimetallic complex **1**. After heterolytic cleavage of the Ru–Mn bond, an epoxide molecule coordinates to the electrophilic ruthenium center through the $O_{(epoxide)}$ atom to afford complex **2** via the transition state $\mathbf{TS_{1-2}}$. In Route I, carbon dioxide then coordinates to the nucleophilic manganese center through the electrophilic carbon atom to form complex **3**. Ring-opening of the epoxide in **3** to form **4** takes place via the transition state $\mathbf{TS_{3-4}}$. In this step, one of the two nucleophilic oxygen atoms of the carboxylate moiety attacks one of the carbon atoms of the coordinated epoxide ring, which behaves as an electrophile, to afford a relatively stable intermediate **4**. Intermediates **4** and **5** are rotational isomers which differ in their O-C-C-O dihedral angles, being −72.5 and 59.3°, respectively. We were unable to locate the rotational transition state because of the flatness of the potential energy surface near the transition state, however, we expect that the rotational barrier is small. From the rotational isomer **5**, ring-closure occurs via $\mathbf{TS_{5-6}}$ to give **6** in which the product molecule (cyclic carbonate) is coordinated to the ruthenium metal center. The last step involves the dissociation of the cyclic carbonate from the ruthenium center and regeneration of the catalyst via transition state $\mathbf{TS_{6-7}}$.

In Route II, after coordination of the epoxide to the ruthenium center to give complex **2**, the nucleophilic manganese center attacks one of the carbon atoms of the ruthenium-coordinated epoxide and opens the epoxide ring to afford a stable alkoxide intermediate **8** via transition state $\mathbf{TS_{2-8}}$. Carbon dioxide interacts with the oxygen atom bonded to the ruthenium center to form **9**. Insertion of the carbon dioxide molecule into the Ru–O bond generates the cyclic metal carbonate **10** via the transition state $\mathbf{TS_{9-10}}$. Intermediates **10** and **11** are rotational isomers with different Ru-O-C=O and O=C-O-C dihedral angles. The Ru-O-C=O dihedral angles of **10** and **11** are 139.9 and 13.4°, respectively, and the O=C-O-C dihedral angles are −7.2 and −173.4°, respectively. Ring-closure of **11** occurs via $\mathbf{TS_{11-6}}$ to give **6** with the cyclic carbonate (the product molecule) coordinated to the ruthenium center through the oxygen atom. Finally, dissociation of the cyclic carbonate from **6** and formation of the Ru–Mn bond regenerates the bimetallic catalyst.

Energetic aspects of Routes I and II: On the basis of the energy profiles shown in Figure 3, we can see that Route I involves two major steps. 1) Coordination of the epoxide to the Lewis acidic ruthenium center with heterolytic cleavage of the Ru–Mn bond and metallocarboxylate-nucleophilic ring-opening of the epoxide. 2) Ring-closure of intermediate **5** to yield the product molecule (cyclic carbonate) and regeneration of the catalyst. Coordination of the epoxide to the ruthenium center and formation of the metallocarboxylate **3** occur sequentially in the first major step leading to a significant decrease in entropy. The Ru–Mn heterolytic cleavage causes charge separation, giving ruthenium a formal charge of +1 and manganese a charge of −1. The charge separation, entropy loss, and opening of the epoxide ring, all together, contribute to a very large barrier (53.91 kcal mol^{-1}, $\mathbf{1}\rightarrow\mathbf{TS_{3-4}}$) to the first major step. In the second major step, ring-closure in **5** to yield the product molecule (cyclic carbonate) again leads to charge separation. This step ($\mathbf{5}\rightarrow\mathbf{TS_{5-6}}$) has a barrier of 35.93 kcal mol^{-1}.

Route II involves three major steps. 1) Coordination of the epoxide to the Lewis acidic ruthenium center with heterolytic cleavage of the Ru–Mn bond and manganese-nucleophilic ring-opening of the epoxide to give **8**. 2) Insertion of CO_2 into the Ru–O bond in **8** to give **10**. 3) Ring-closure in **10** to yield the cyclic carbonate and regeneration of the catalyst. The first major step has an overall energy barrier of 44.04 kcal mol^{-1}, which is less than the overall barrier calculated for the first major step of Route I. The energy required for coordination of the epoxide and heterolytic cleavage of the Ru–Mn bond is the same as that in Route I. The smaller overall barrier here is a result of a smaller barrier to manganese-nucleophilic ring-opening than that for the metallocarboxylate-nucleophilic ring-opening of Route I. By examining the energy changes for the steps $\mathbf{2}\rightarrow\mathbf{TS_{2-8}}$ and $\mathbf{2}\rightarrow\mathbf{TS_{3-4}}$, we can conclude that the unfavorable metallocarboxylate-nucleophilic ring-opening in Route I is mainly related to an entropy effect. In Route II, ring-opening occurs immediately after the heterolytic Ru–Mn bond cleavage. However, the ring-opening in Route I occurs after **2** has taken up one more molecule, CO_2. The insertion of CO_2 into **8** in the second major step does not cost much energy with an energy barrier of 24.68 kcal mol^{-1}. In the third major step, ring-closure in **10** to yield the product molecule (cyclic carbonate), similar to the second major step in Route I, has a large barrier of 44.59 kcal mol^{-1} (from **10** to $\mathbf{TS_{11-6}}$). Again, formation of **6** causes charge separation between the two metal centers, contributing to the large barrier. As the difference in the overall energy barriers between the first and third major steps is small, we expect that these two steps are important in determining the reaction rate.

By comparing the energetics of Routes I and II described above, one finds that Route II is favored over Route I. The experiments described in the preceding section show that the presence of electron-withdrawing groups on the epoxides leads to higher conversions (Table 4). It is expected that electron-withdrawing groups, which increase the electrophilicity of the epoxide carbon atoms, should reduce the barrier to the manganese-nucleophilic ring-opening step in Route II. Electron-withdrawing groups should also facilitate the ring-closure in **11** because this step is also related to the electrophilic attack of one of the epoxide carbon atoms on the ruthenium-bonded oxygen in **11**.

Note that the reaction barriers calculated for both Routes I and II are very high. As mentioned above and as will be discussed in more detail below, the reaction paths involve heterolytic Ru–Mn bond cleavage which causes charge separation. It is well recognized that gas-phase calculations, which are now commonly carried out in computational chemistry, for such charge separation processes always produce very high reaction barriers.[26] Since we are interested in the comparison of Routes I and II, the relative barrier heights are more important than the absolute barriers. Note

also that intermediates **8**–**10** were predicted by the calculations to be stable. However, we did not observe these species experimentally. We suspect that the calculations might have overestimated the electrostatic interactions between ruthenium and oxygen and between manganese and carbon atoms in the Ru–O and Mn–C bonds of the intermediates, again because gas-phase models were used.

Structures of the species in Route II: Structural details of the optimized intermediates and transition states of the favored route (Route II) are shown in Figure 4. Complex **1** can be described as being composed of a square pyramidal 18-electron Mn^{-I} d^8ML_5 anion coordinated to a 16-electron Ru^{II} d^6-$CpML_2$ cation fragment through a dative Ru←Mn bond. The calculated bond length of Ru–Mn in **1** is 2.933 Å, which is slightly longer than the corresponding bond length (2.852 Å) in the X-ray crystal structure reported in Table 2. The metal–phosphine and metal–carbonyl distances are well-reproduced. The calculated bond lengths and bond angles of **1** are in reasonably good agreement with the ex-

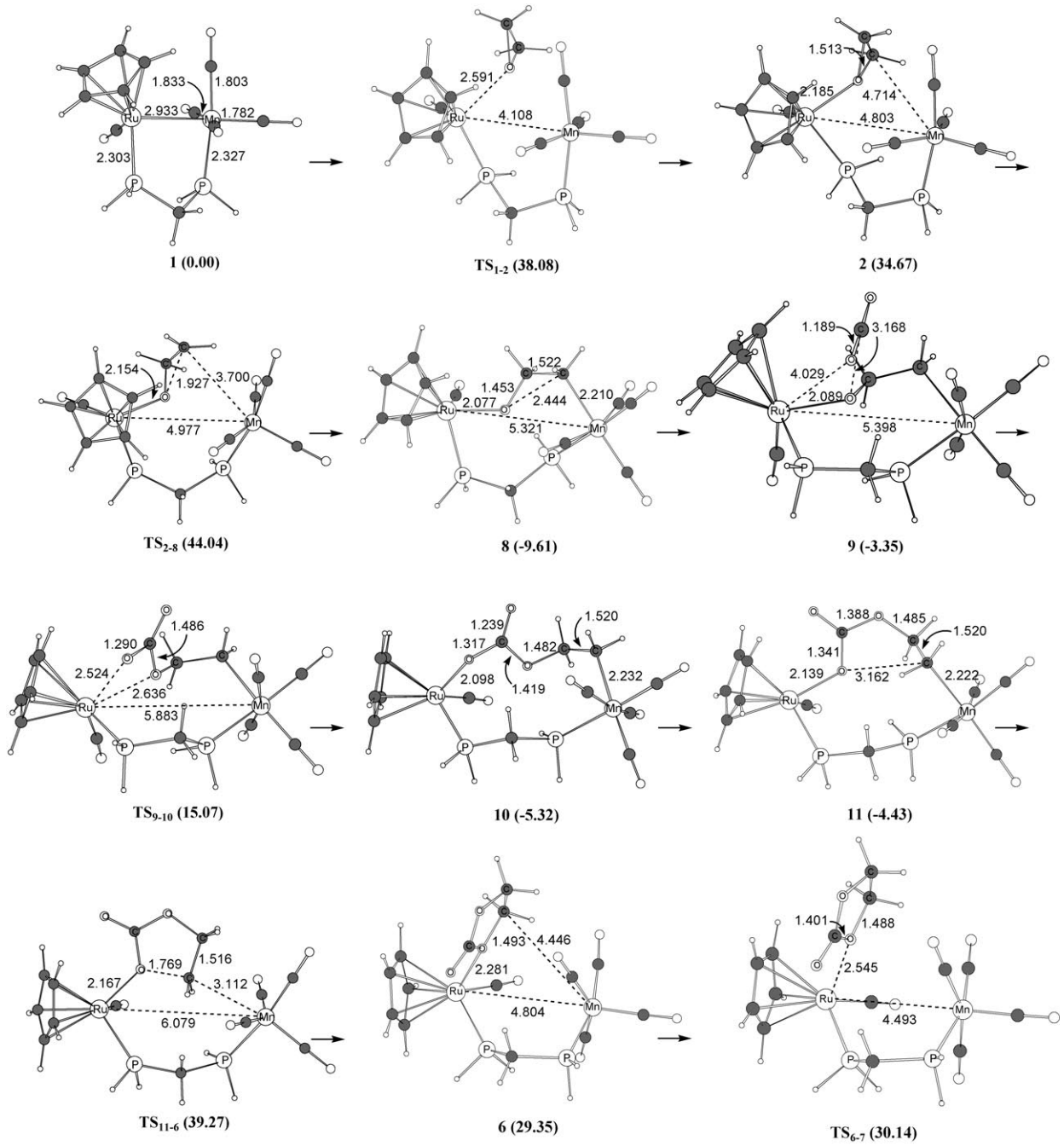

Figure 4. B3LYP-optimized structures for the species shown in Figure 3 (Route II). The free energies (kcal mol^{-1}) relative to the reactants are given in parentheses. Bond lengths are given in angstroms.

perimental values. In **2**, the Ru–Mn distance is considerably lengthened to 4.803 Å, indicating that the Ru–Mn bond is completely broken. The calculated NBO natural charges[27] of the ruthenium and manganese centers are 0.12 and −0.86, respectively, suggesting that **2** more closely resembles a ruthenium cation/manganese anion pair. Heterolytic bond cleavage in the gas-phase requires a huge amount of energy, therefore, the high activation barrier for the process **1**→**2** is reasonable. In the transition state $\mathbf{TS_{2-8}}$, the $O_{(epoxide)}$–$C_{(epoxide)}$ bond is lengthened to 1.927 Å and the $C_{(epoxide)}$···Mn distance is reduced to 3.700 Å. These features indicate that $\mathbf{TS_{2-8}}$ is an early transition state. The ruthenium and manganese centers in **8** are bridged by an alkoxide group. In the transition state $\mathbf{TS_{9-10}}$, the $C_{(CO_2)}$–$O_{(epoxide)}$ and Ru–$O_{(CO_2)}$ distances are shortened to 1.486 and 2.524 Å, respectively, and the $C_{(CO_2)}$–$O_{(CO_2)}$ and Ru–$O_{(epoxide)}$ bonds are lengthened to 1.290 and 2.636 Å, respectively. These geometrical features indicate that $\mathbf{TS_{9-10}}$ is a concerted four-center transition state. In the intermediate **10**, the ruthenium and manganese centers are bridged by the carbonate group. From **10** to **11**, the Ru–O–C=O dihedral angle changes from 139.9 to 13.4°, so that the lone pairs of the oxygen atom, which is bonded to the ruthenium atom, are ready to interact with one of the carbon atoms of the epoxide in the transition state $\mathbf{TS_{11-6}}$ in the ring-closure process. In the transition state $\mathbf{TS_{11-6}}$, the Mn–$C_{(epoxide)}$ distance is lengthened to 3.112 Å and the $C_{(epoxide)}$–$O_{(CO_2)}$ distance shortened to 1.769 Å, typical of a late transition state. In **6**, the Mn–$C_{(epoxide)}$ and Ru–Mn distances are 4.446 and 4.804 Å, respectively, indicating that there is no bonding interaction between the ruthenium and manganese fragments. The calculated NBO natural charges[27] of the ruthenium and manganese centers are 0.10 and −0.88, respectively. Similar to the process of **1**→**2**, heterolytic bond cleavage occurs in the **11**→**6** process, requiring a high activation barrier. In the transition state $\mathbf{TS_{6-7}}$, the Ru–Mn distance is shortened to 4.493 Å and the Ru–O distance is lengthened to 2.545 Å. This transition state is related to dissociation of the product molecule (cyclic carbonate) and regeneration of the catalyst.

Conclusions

This work reports catalytic CO_2/epoxide coupling reactions with well-defined heterobimetallic complexes. Our study indicates that cooperative participation of the metal centers of the complexes occurs during the catalytic process. Theoretical calculations seem to support a reaction pathway involving heterolytic cleavage of the Ru–Mn bond and epoxide coordination to the Lewis acidic ruthenium center, ring-opening of the epoxide by the Lewis basic manganese center followed by CO_2 insertion into the Ru–O bond to afford the carbonato intermediate, which then undergoes ring-closure to yield the cyclic carbonate product. The heterolytic metal–metal bond cleavage and the ring-closure steps, both of which cause charge separations, have high energy barriers.

Experimental Section

All experiments were carried out under dry nitrogen using standard Schlenk techniques. All solvents were distilled and degassed prior to use. Dichloromethane was distilled from calcium hydride. Tetrahydrofuran, diethyl ether, toluene, and hexane were distilled from sodium-benzophenone ketyl. Methanol and ethanol were distilled from magnesium and iodine. $[Mn_2(CO)_{10}]$ was purchased from Strem. $Li(C_2H_5)_3BH$ was purchased from Aldrich. $[Mn_2(CO)_8(PPh_3)_2]$,[28] $Li[Mn(CO)_5]$,[29] $[(\eta^5\text{-}C_5H_5)Ru(dppm)Cl]$,[30] $[(\eta^5\text{-}C_5H_5)Ru(dppm)H]$,[31] $[\eta^5\text{-}C_5(CH_3)_5]Ru(dppm)Cl]$,[8] $[\eta^5\text{-}C_5(CH_3)_5]Ru(dppm)H]$,[8] $[(\eta^5\text{-}C_5H_5)Ru(CO)(dppm)]I$,[32] and $[(\eta^5\text{-}C_5H_5)Ru(CO)(PPh_3)(CH_3CN)]BF_4$[33] were prepared according to published procedures. $[HMn(CO)_5]$ was synthesized according to a literature procedure except that $Li(C_2H_5)_3BH$ was used instead of Na/Hg.[34] Propylene oxide and butadiene monoxide were purchased from Aldrich. Epifluorohydrin, epichlorohydrin, styrene oxide, cyclohexene oxide, isobutylene oxide, and 1,2-epoxyhexane were purchased from Acros. All substrates were dried with molecular sieves before use.

Infrared spectra were recorded with a Bruker Vector 22 FT-IR spectrophotometer. ^1H NMR spectra were recorded with a Bruker DPX 400 spectrometer at 400.13 MHz. Chemical shifts (δ, ppm) were measured relative to the proton residue of the deuteriated solvent ([D$_8$]THF: δ = 1.85 ppm, C_6D_6: δ = 7.40 ppm). $^{31}P\{^1H\}$ NMR spectra were recorded with a Bruker DPX-400 spectrometer at 161.98 MHz. The chemical shifts are referenced to external 85 % H_3PO_4 in D_2O (δ = 0.0 ppm). $^{13}C\{^1H\}$ NMR spectra were recorded with a Bruker DPX-400 spectrometer at 100.63 MHz. High-pressure NMR studies were carried out in a sapphire NMR tube; the 10 mm sapphire NMR tube was purchased from Saphikon, Milford, NH, USA, and the titanium high-pressure valve was constructed at the ISSECC-CNR, Firenze, Italy. Mass Spectrometry was carried out with a Finnigan MAT 95S mass spectrometer. Elemental analyses were performed by M-H-W Laboratories, Phoenix, AZ, USA.

$[(\eta^5\text{-}C_5H_5)Ru(CO)(\mu\text{-}dppm)Mn(CO)_4]$ (1a) by H_2 elimination: A THF (15 mL) solution of $[HMn(CO)_5]$ (0.032 g, 0.163 mmol) was transferred into a Schlenk flask equipped with a water condenser and loaded with a sample of $[(\eta^5\text{-}C_5H_5)Ru(dppm)H]$ (0.090 g, 0.163 mmol). The resulting mixture was refluxed for 24 h. After cooling to room temperature, the solvent was removed under vacuum to afford an orange paste. Hexane (5 mL) was added, with stirring, to obtain an orange solid which was washed with diethyl ether (1 mL) and hexane (2 mL) and then dried in vacuo for 6 h. Yield: 0.099 g (82 %). Elemental analysis calcd (%) for $C_{35}H_{27}O_5P_2RuMn$: C 56.39, H 3.65; found: C 56.29, H 3.61; IR (KBr): $\tilde{\nu}$(C≡O) = 1710 (m), 1896 (s), 1938 (s), and 2000 cm^{-1} (s); ^1H NMR (400.13 MHz, C_6D_6, 25 °C): δ = 2.90 (t, J(H,P) = 9.91 Hz, 2H; PCH_2P), 5.02 (s, 5H; Cp), 7.72–7.13 ppm (m, 20H of dppm); $^{31}P\{^1H\}$ NMR (161.98 MHz, C_6D_6, 25 °C): δ = 54.9 (d, J(P,P) = 91.2 Hz), 56.5 ppm (d, J(P,P) = 91.2 Hz); ESI-MS (CH_2Cl_2/MeOH as solvent): m/z: 746 $[M]^+$.

$[(\eta^5\text{-}C_5H_5)Ru(CO)(\mu\text{-}dppm)Mn(CO)_4]$ (1a) by metathetical reaction: A THF solution (10 mL) solution of $Li^+[Mn(CO)_5]^-$ (0.060 g, 0.295 mmol) was transferred with a cannula into a Schlenk flask equipped with a water condenser and loaded with a sample of $[(\eta^5\text{-}C_5H_5)Ru(dppm)Cl]$ (0.173 g, 0.295 mmol). The mixture was refluxed for 24 h. After cooling the solution to room temperature, the solvent was removed under vacuum to yield a crude orange solid. Toluene (8 mL) was added to the solid and the resulting mixture was filtered through Celite to remove the salt. The solvent of the filtrate was removed by vacuum to give an orange paste which was washed with diethyl ether (1 mL) and hexanes (2 mL) and dried in vacuum for 6 h to afford the pure product. Yield: 0.176 g (80 %). The IR, NMR, and mass spectrometric data of the product were identical to those of the product obtained by the synthetic method described above.

$[\{\eta^5\text{-}C_5(CH_3)_5\}Ru(\mu\text{-}CO)_2(\mu\text{-}dppm)Mn(CO)_3]$ (1b) by H_2 elimination: This complex was prepared by using the same procedure as described above for the preparation of **1a** except $[\{\eta^5\text{-}C_5(CH_3)_5\}Ru(dppm)H]$ was used in place of $[(\eta^5\text{-}C_5H_5)Ru(dppm)H]$. Yield: 0.059 g (83 %). Elemental analysis calcd (%) for $C_{40}H_{37}O_5P_2RuMn$: C 58.90, H 4.57; found: C 58.77, H 4.61; IR (KBr): $\tilde{\nu}$(C≡O) = 1710 (m), 1892 (s), 1912 (s), 1989 cm^{-1} (s); ^1H NMR (C_6D_6, 400.13 MHz, 25 °C): δ = 1.76 (s, 15H; methyls of Cp*),

2.35 (t, J(H,P) = 9.1 Hz, 2H; PCH_2P), 7.66–7.04 ppm (m, 20H of dppm); $^{31}P\{^1H\}$ NMR (C_6D_6, 161.98 MHz, 25 °C): δ = 48.1 (d, J(P,P) = 105.0 Hz), 51.2 ppm (d, J(P,P) = 105.0 Hz); ESI-MS (CH_2Cl_2/MeOH): m/z: 816 $[M]^+$.

[{η⁵-C₅(CH₃)₅}Ru(μ-CO)₂(μ-dppm)Mn(CO)₃] (1b) by metathetical reaction: Complex **1b** was synthesized by using the same procedure as described above for the preparation of **1a** by the same method except that [{η⁵-$C_5(CH_3)_5$}Ru(dppm)Cl] was used instead of [(η⁵-C_5H_5)Ru(dppm)Cl]. Yield: 0.109 g (83%).

H/D exchange between [(η⁵-C₅R₅)Ru(dppm)D] (R = H, CH₃) and [HMn(CO)₅]: In a typical experiment, the ruthenium deuteride complex (0.006 mmol) was loaded into a 5-mm NMR tube which was then sealed with a rubber septum. The tube was purged and filled with nitrogen. Degassed [D_8]THF (0.4 mL) was added through a syringe to dissolve the complex. A [D_8]THF solution (0.4 mL) of [$HMn(CO)_5$] (0.006 mmol) was added to the tube using a syringe and a needle. The ^1H NMR spectrum of the mixture was recorded immediately at room temperature.

Li[Mn(CO)₄(PPh₃)] (1c): A sample of [$Mn_2(CO)_8(PPh_3)_2$] (0.15 g, 0.17 mmol) was dissolved in THF (10 mL) in a 50 mL Schlenk flask. Excess $Li(C_2H_5)_3BH$ (1.0 M solution in THF, 0.44 mL, 0.44 mmol, 2.5 equiv) was added slowly to this solution, which was cooled to 0 °C, using a syringe and a needle over a period of 20 min. The solution was stirred for 2.5 h, during which time the temperature of the reaction mixture gradually increased to room temperature. The solvent was then removed under vacuum to afford a crude yellow solid which was washed with diethyl ether (3 mL). The residue was then extracted with toluene (5 mL) and the solvent of the extract was removed under vacuum to yield a yellow solid which was washed with hexane (5 mL) and dried in vacuo. Yield: 0.10 g (74%). IR (KBr): $\tilde{\nu}$(C≡O) = 1890 (sh), 1904 (s), 1996 cm^{-1} (m); ^1H NMR (400.13 MHz, [D_8]THF, 25 °C): δ = 7.44–7.84 ppm (m, H atoms of PPh_3); $^{31}P\{^1H\}$ NMR (161.98 MHz, [D_8]THF, 25 °C): δ = 74.67 ppm (s); ESI-MS (CH_2Cl_2/MeOH): m/z: 429 $[M-Li]^+$.

Catalytic coupling reactions of CO_2 with epoxides: The reactions were carried out in a 40-mL stainless steel autoclave. In a typical run, the complex (3.5 μmol) was dissolved in the epoxide (31.5 mmol) and the solution was heated under 40 bar of CO_2 at 100 °C for 45 h. The reactor was cooled rapidly in an ice-bath and carefully vented. The cyclic carbonates formed were isolated by vacuum distillation and analyzed by ^1H NMR spectroscopy.

Crystallographic analysis of [(η⁵-C₅H₅)Ru(CO)(μ-dppm)Mn(CO)₄] (1a) and [{η⁵-C₅(CH₃)₅}Ru(μ-CO)₂(μ-dppm)Mn(CO)₃] (1b): Crystals of **1a** and **1b** suitable for X-ray diffraction studies were obtained by layering hexane on CH_2Cl_2 solutions of the complexes. A suitable crystal of **1a** or **1b** was mounted on a Bruker CCD area detector diffractometer and subjected to $Mo_{K\alpha}$ radiation (λ = 0.71073 Å) from a generator operating at 50 kV and 30 mA. The intensity data of **1a** and **1b** were collected in the range of 2θ = 3–55° with oscillation frames of ϕ and ω in the range of 0–180°; 1321 frames were recorded in four shells. An empirical absorption correction based on Fourier coefficient fitting was applied using the SADABS program (Sheldrick, 1996). The crystal structures were determined by direct methods, which yielded the positions of some of the non-hydrogen atoms, and subsequent difference Fourier syntheses were employed to locate all of the remaining non-hydrogen atoms that did not show up in the initial structure. Hydrogen atoms were located based on difference Fourier syntheses connecting geometrical analysis. All non-hydrogen atoms were refined anisotropically with a weight function of $w = 1/[\sigma^2(F_o^2) + 0.1000p]^2 + 0.0000p$, where $p = (F_o^2 + 2F_c^2)/3$. Hydrogen atoms were refined with fixed individual displacement parameters. All experiments and computations were performed with a Bruker CCD area detector diffractometer and a PC computer using the Bruker Smart and Bruker SHELXTL packages.

Computational details: Density functional theory calculations at the Becke3LYP (B3LYP) level of theory[35] were used to optimize the geometries of all the reactants, intermediates and transition states. Frequency calculations at the same level of theory were also performed to identify all stationary points as minima (zero imaginary frequency) or transition states (one imaginary frequency). Intrinsic reaction coordinates (IRC)[36] were also calculated for the transition states to confirm that such structures indeed connect two minima. The effective core potentials (ECPs) of Hay and Wadt with a double-ζ valence basis set (LanL2DZ)[37] were used to describe ruthenium, manganese, and phosphorus atoms. For all the other atoms, the standard 6-31G basis set[38] was used. Polarization functions were added for the ruthenium [ζ_f(Ru) = 1.235], manganese [ζ_f(Mn) = 2.195],[39] and phosphorus [ζ_d(P) = 0.340] atoms.[40] All calculations were performed by using the Gaussian 03 software package[41] on PC Pentium IV computers.

CCDC-276203 (**1a**) and CCDC-276204 (**1b**) contain the supplementary crystallographic data for this paper. These data can be obtained free of charge from The Cambridge Crystallographic Data Centre via www.ccdc.cam.ac.uk/data_request/cif.

Acknowledgements

We thank the Hong Kong Research Grant Council (Project Nos. PolyU 5282/02P, PolyU 5006/03P, and HKUST6023/04P) for financial support.

[1] See, for example: a) F. Torres, E. Sola, A. Elduque, A. R. Martinez, F. J. Lohoz, L. A. Oro, *Chem. Eur. J.* **2000**, *6*, 2120–2128; b) Y. Yuan, M. V. Jiménez, E. Sola, F. J. Lahoz, L. A. Oro, *J. Am. Chem. Soc.* **2002**, *124*, 752–753; c) R. C. Mathews, D. K. Howell, W.-J. Peng, S. G. Train, W. D. Treleaven, G. G. Stanley, *Angew. Chem.* **1996**, *108*, 2402–2405; *Angew. Chem. Int. Ed. Engl.* **1996**, *35*, 2253–2256; d) M. E. Broussard, B. Juma, S. G. Train, W. Peng, S. A. Laneman, G. G. Stanley, *Science* **1993**, *260*, 1784–1788; e) J. R. Torkelson, F. H. Antwi-Nsiah, R. McDonald, M. Cowie, J. G. Pruis, K.-J. Jalkanen, R. L. DeKock, *J. Am. Chem. Soc.* **1999**, *121*, 3666–3683; f) J. R. Torkelson, R. McDonald, M. Cowie, *J. Am. Chem. Soc.* **1998**, *120*, 4047–4048; g) M. M. Dell′Anna, S. J. Trepanier, R. McDonald, M. Cowie, *Organometallics* **2001**, *20*, 88–99; h) Y. Ohki, H. Suzuki, *Angew. Chem.* **2000**, *112*, 3605–3607; *Angew. Chem. Int. Ed.* **2000**, *39*, 3463–3465; i) T. Shima, H. Suzuki, *Organometallics* **2000**, *19*, 2420–2422; j) K. Tada, M. Oishi, H. Suzuki, *Organometallics* **1996**, *15*, 2422–2424; k) M. D. Fryzuk, S. A. Johnson, B. O. Patrick, A. Albinati, S. A. Mason, T. F. Koetzle, *J. Am. Chem. Soc.* **2001**, *123*, 3960–3973.

[2] a) R. D. Adams, F. A. Cotton, *Catalysis by Di- and Polynuclear Metal Complexes*, Wiley-VCH, New York, **1998**; b) P. Braunstein, J. Rose in *Comprehensive Organometallic Chemistry, Vol. 10*, 2nd ed. (Eds.: E. W. Abel, F. G. A. Stone, G. Wilkinson), Pergamon Press, Oxford, **1995**, Chapter 7.

[3] a) L. H. Gade, *Angew. Chem.* **2000**, *112*, 2768–2789; *Angew. Chem. Int. Ed.* **2000**, *39*, 2659–2678; b) L. H. Gade, H. Memmler, U. Kauper, A. Schneider, S. Fabre, I. Bezongli, M. Lutz, C. Galka, I. J. Scowen, M. McPartlin, *Chem. Eur. J.* **2000**, *6*, 692–708; c) S. Tsutsuminai, N. Komine, M. Hirano, S. Komiya, *Organometallics* **2003**, *22*, 4238–4247; d) K. Uehara, S. Hikichi, M. Akita, *Organometallics* **2001**, *20*, 5002–5004; e) W. C. Mercer, R. R. Whittle, E. W. Burkhardt, G. L. Geoffroy, *Organometallics* **1985**, *4*, 68–74; f) D. A. Roberts, W. C. Mercer, S. M. Zahurak, G. L. Geoffroy, C. W. DeBrosse, M. E. Cass, C. G. Pierpont, *J. Am. Chem. Soc.* **1982**, *104*, 910–913.

[4] a) W. Leitner, *Coord. Chem. Rev.* **1996**, *155*, 257–284; b) T. J. Marks, *Chem. Rev.* **2001**, *101*, 953–996.

[5] a) A. Behr, *Angew. Chem.* **1988**, *100*, 681–698; *Angew. Chem. Int. Ed. Engl.* **1988**, *27*, 661–678; b) A.-A. Shaikh, S. Sivaram, *Chem. Rev.* **1996**, *96*, 951–976.

[6] See, for example: a) R. L. Paddock, S. T. Nguyen, *J. Am. Chem. Soc.* **2001**, *123*, 11498–11499; b) K. Yamaguchi, K. Ebitani, T. Yoshida, H. Yoshida, K. Kaneda, *J. Am. Chem. Soc.* **1999**, *121*, 4526–4527; c) T. Yano, H. Matsui, T. Koiki, H. Ishiguro, H. Fujihara, M. Yoshihara, T. Maeshima, *Chem. Commun.* **1997**, 1129–1130; d) D. J. Darensbourg, M. W. Holtcamp, *Coord. Chem. Rev.* **1996**, *153*, 155–174; e) T. Fujinami, T. Suzuki, M. Kamiya, S. Fukuzawa, S. Sakai, *Chem. Lett.* **1985**, 199–200; f) H. S. Kim, J. J. Kim, B. G. Lee, O. S.

Jung, H. G. Jang, S. O. Kang, *Angew. Chem.* **2000**, *112*, 4262–4264; *Angew. Chem. Int. Ed.* **2000**, *39*, 4096–4098; g) W. J. Kruper, D. V. Deller, *J. Org. Chem.* **1995**, *60*, 725–727; h) V. Caló, A. Nacci, A. Monopoli, A. Fanizzi, *Org. Lett.* **2002**, *4*, 2561–2563; i) H. Kawanami, Y. Ikushima, *Chem. Commun.* **2000**, 2089–2090; j) N. Kihara, N. Hara, T. Endo, *J. Org. Chem.* **1993**, *58*, 6198–6202; k) F. Li, C. Xia, L. Xu, W. Sun, G. Chen, *Chem. Commun.* **2003**, 2042–2043; l) X.-B. Lu, B. Liang, Y.-J. Zhang, Y.-Z. Tian, Y.-M. Wang, C.-X. Bai, H. Wang, R. Zhang, *J. Am. Chem. Soc.* **2004**, *126*, 3732–3733; m) Y.-M. Shen, W.-L. Duan, M. Shi, *J. Org. Chem.* **2003**, *68*, 1559–1562; n) F. Li, L. Xiao, C. Xia, B. Hu, *Tetrahedron Lett.* **2004**, *45*, 8307–8310; o) J.-L. Jiang, F. Gao, R. Hua, X. Qiu, *J. Org. Chem.* **2005**, *70*, 381–383.

[7] S. S. Kristjándóttir, J. R. Norton, *Transition Metal Hydrides* (Ed.: A. Dedieu), VCH, Weinheim, **1992**.

[8] G. Jia, R. H. Morris, *J. Am. Chem. Soc.* **1991**, *113*, 875–883.

[9] For dihydrogen bonding, see: a) R. H. Crabtree, P. E. M. Siebbahn, O. Eisenstein, A. L. Rheingold, T. F. Koetzle, *Acc. Chem. Res.* **1996**, *29*, 348–354; b) R. H. Crabtree, *Science* **1998**, *282*, 2000–2001; c) R. Custelcean, J. E. Jackson, *Chem. Rev.* **2001**, *101*, 1963–1980.

[10] M. S. Chinn, D. M. Heinekey, *J. Am. Chem. Soc.* **1990**, *112*, 5166–5175.

[11] a) H. Matsuzaka, K. Ichikawa, T. Ishii, M. Kondo, S. Kitagana, *Chem. Lett.* **1998**, 1125–1126; b) L. Carlton, W. E. Lindsell, K. J. McCullough, P. N. Preston, *J. Chem. Soc. Chem. Commun.* **1982**, 1001–1003; c) C. P. Casey, Y. Wang, R. S. Tanke, P. N. Hazin, E. W. Rutter, Jr., *New. J. Chem.* **1994**, *18*, 43–50.

[12] M. L. Man, Z. Zhou, S. M. Ng, C. P. Lau, *Dalton Trans.* **2003**, 3727–3735.

[13] D. M. Antonelli, M. Cowie, *Organometallics* **1990**, *9*, 1818–1826.

[14] C. P. Casey, R. M. Bullock, F. Nief, *J. Am. Chem. Soc.* **1983**, *105*, 7574–7580.

[15] A. J. M. Caffyn, M. J. Mays, P. R. Raithby, *J. Chem. Soc. Dalton Trans.* **1991**, 2349–2356.

[16] H. A. Nieuwenhuis, A. V. Loon, M. A. Moraal, D. J. Stufkens, A. Oskam, K. Goubitz, *Inorg. Chim. Acta* **1995**, *232*, 19–25.

[17] C. P. Casey, R. E. Palermo, R. F. Jordan, *J. Am. Chem. Soc.* **1985**, *107*, 4597–4599.

[18] H. S. Chu, C. P. Lau, K. Y. Wong, W. T. Wong, *Organometallics* **1998**, *17*, 2768–2777.

[19] a) C. Yin, Z. Xu, S.-Y. Yang, S. M. Ng, K. Y. Wong, Z. Lin, C. P. Lau, *Organometallics* **2001**, *20*, 1216–1222; b) S. M. Ng, C. Yin, C. H. Yeung, T. C. Chan, C. P. Lau, *Eur. J. Inorg. Chem.* **2004**, 1788–1793.

[20] a) Y. Blum, D. Czarkie, Y. Rahamin, Y. Shvo, *Organometallics* **1985**. *4*, 1459–1461; b) Y. Shvo, D. Czarkie, Y. Rahamin, *J. Am. Chem. Soc.* **1986**, *108*, 7400–7403; c) N. Menashe, Y. Shvo, *Organometallics* **1991**, *10*, 3885–3891; d) N. Menashe, E. Salant, Y. Shvo, *J. Organomet. Chem.* **1996**, *514*, 97–102; e) C. P. Casey, S. W. Singer, D. R. Powell, R. K. Hayashi, M. Kavana, *J. Am. Chem. Soc.* **2001**, *123*, 1090–1100; f) B. A. Persson, A. L. E. Larsson, M. LeRay, J. E. Bäckvall, *J. Am. Chem. Soc.* **1999**, *121*, 1645–1650; g) G. Csjernyik, A. H. Éll, L. Fadini, B. Pugin, J. E. Bäckvall, *J. Org. Chem.* **2002**, *67*, 1657–1662.

[21] a) K.-J. Haack, S. Hashiguchi, A. Fujii, T. Ikariya, R. Noyori, *Angew. Chem.* **1997**, *109*, 297–300; *Angew. Chem. Int. Ed. Engl.* **1997**, *36*, 285–288; b) M. Yamakawa, I. Yamada, R. Noyori, *Angew. Chem.* **2001**, *113*, 2900–2903; *Angew. Chem. Int. Ed.* **2001**, *40*, 2818–2821.

[22] K. Abdar-Rashid, M. Faatz, A. J. Lough, R. H. Morris, *J. Am. Chem. Soc.* **2001**, *123*, 7473–7474.

[23] D. H. Gibson, T.-S. Ong, *J. Am. Chem. Soc.* **1987**, *109*, 7191–7193.

[24] a) L. E. Martínez, J. L. Leighton, D. H. Carsten, E. N. Jacobsen, *J. Am. Chem. Soc.* **1995**, *117*, 5897–5898; b) K. B. Hansen, J. L. Leighton, E. N. Jacobsen, *J. Am. Chem. Soc.* **1996**, *118*, 10924–10925; c) P. Tascedda, M. Weidmann, E. Dinjus, E. Duñach, *Appl. Organomet. Chem.* **2001**, *15*, 141–144; d) V. Mahaderan, Y. D. Y. L. Getzler, G. W. Coates, *Angew. Chem.* **2001**, *113*, 2211–2214; *Angew. Chem. Int. Ed.* **2001**, *40*, 2781–2784; e) see reference [6f]; f) H. S. Kim, J. J. Kim, S. D. Lee, M. S. Lah, D. Moon, H. G. Jang, *Chem. Eur. J.* **2003**, *9*, 678–686.

[25] a) T. Tsuda, S. I. Sanada, K. Ueda, T. Saegusa, *Inorg. Chem.* **1976**, *15*, 2329–2332; b) D. J. Darensbourg, M. W. Holtcamp, G. E. Struck, M. S. Zimmer, S. A. Niezgoda, P. Rainey, J. B. Robertson, J. D. Draper, J. H. Reibenspies, *J. Am. Chem. Soc.* **1999**, *121*, 107–116.

[26] J. G. Cordaro, R. G. Bergman, *J. Am. Chem. Soc.* **2004**, *126*, 16912–16929.

[27] E. D. Glendening, A. E. Reed, J. E. Carpenter, F. Weihold, NBO, Version 3.1.

[28] D. Drew, D. J. Darensbourg, M. Y. Darensbourg, *Inorg. Chem.* **1975**, *14*, 1579–1584.

[29] J. A. Gladysz, G. M. Williams, W. Tam, D. L. Johnson, D. W. Parker, J. C. Selover, *Inorg. Chem.* **1979**, *18*, 553–558.

[30] a) M. I. Bruce, C. Hameisten, A. G. Swincer, R. C. Wallis, *Inorg. Synth.* **1982**, *21*, 78–84; b) R. B. King, F. G. A. Stone, *Inorg. Synth.* **1963**, *7*, 99–115.

[31] L. Ballester, A. Gutierrez, M. F. Perpinan, *J. Chem. Educ.* **1989**, *66*, 777–778.

[32] N. J. Coville, E. A. Darling, *J. Organomet. Chem.* **1984**, *260-278*, 105–111.

[33] P. M. Treichel, D. A. Komer, *Synth. React. Inorg. Met.-Org. Chem.* **1980**, *10*, 205–218.

[34] E. A. McNeill, F. R. Scholer, *J. Am. Chem. Soc.* **1977**, *99*, 6243–6249.

[35] a) A. D. Becke, *Phys. Rev. A* **1988**, *38*, 3098–3100; b) A. D. Becke, *J. Chem. Phys.* **1993**, *98*, 5648–5652; c) B. Miehlich, A. Savin, H. Stoll, H. Preuss, *Chem. Phys. Lett.* **1989**, *157*, 200–206; d) C. T. Lee, W. T. Yang, R. G. Parr, *Phys. Rev. B* **1988**, *37*, 785–789.

[36] a) K. Fukui, *J. Phys. Chem.* **1970**, *74*, 4161–4163; b) K. Fukui, *Acc. Chem. Res.* **1981**, *14*, 363–368.

[37] a) P. J. Hay, W. R. Wadt, *J. Chem. Phys.* **1985**, *82*, 270–283; b) W. R. Wadt, P. J. Hay, *J. Chem. Phys.* **1985**, *82*, 284–298; c) P. J. Hay, W. R. Wadt, *J. Chem. Phys.* **1985**, *82*, 299–310.

[38] a) M. S. Gordon, *Chem. Phys. Lett.* **1980**, *76*, 163–168; b) P. C. Hariharan, J. A. Pople, *Theor. Chim. Acta* **1973**, *28*, 213–222; c) R. C. Binning, Jr., L. A. Curtiss, *J. Comput. Chem.* **1990**, *11*, 1206–1216.

[39] A. W. Ehlers, M. Bohme, S. Dapprich, A. Gobbi, A. Hollwarth, V. Jonas, K. F. Kohler, R. Stegmann, A. Veldkamp, G. Frenking, *Chem. Phys. Lett.* **1993**, *208*, 111–114.

[40] S. Huzinaga, *Gaussian Basis Sets for Molecular Calculations*, Elsevier Science, Amsterdam, **1984**.

[41] Gaussian 03 (Revision B05), M. J. Frisch, G. W. Trucks, H. B. Schlegel, G. E. Scuseria, M. A. Robb, J. R. Cheeseman, J. A. Montgomery, T. Vreven, Jr., K. N. Kudin, J. C. Burant, J. M. Millam, S. S. Iyengar, J. Tomasi, V. Barone, B. Mennucci, M. Cossi, G. Scalmani, N. Rega, G. A. Petersson, H. Nakatsuji, M. Hada, M. Ehara, K. Toyota, R. Fukuda, J. Hasegawa, M. Ishida, T. Nakajima, Y. Honda, O. Kitao, H. Nakai, M. Klene, X. Li, J. E. Knox, H. P. Hratchian, J. B. Cross, C. Adamo, J. Jaramillo, R. Gomperts, R. E. Stratmann, O. Yazyev, A. J. Austin, R. Cammi, C. Pomelli, J. W. Ochterski, P. Y. Ayala, K. Morokuma, G. A. Voth, P. Salvador, J. J. Dannenberg, V. G. Zakrzewski, S. Dapprich, A. D. Daniels, M. C. Strain, O. Farkas, D. K. Malick, A. D. Rabuck, K. Raghavachari, J. B. Foresman, J. V. Ortiz, Q. Cui, A. G. Baboul, S. Clifford, J. Cioslowski, B. B. Stefanov, G. Liu, A. Liashenko, P. Piskorz, I. Komaromi, R. L. Martin, D. J. Fox, T. Keith, M. A. Al-Laham, C. Y. Peng, A. Nanayakkara, M. Challacombe, P. M. W. Gill, B. Johnson, W. Chen, M. W. Wong, C. Gonzalez, J. A. Pople, Gaussian, Inc., Pittsburgh, PA, **2003**.

Received: July 6, 2005
Published online: October 24, 2005

